Vol. 703: 17–30, 2023
https://doi.org/10.3354/meps14213

MARINE ECOLOGY PROGRESS SERIES
Mar Ecol Prog Ser

Published January 12

Chemical and biological vertical distributions within central Arctic (>82° N) sea ice during late summer

A. Torstensson[1,2,4,*], G. M. Showalter[1], A. R. Margolin[3], E. H. Shadwick[3,5], J. W. Deming[1], W. O. Smith Jr.[3,6]

[1]School of Oceanography, University of Washington, Seattle, WA 98195, USA
[2]Department of Ecology and Genetics, Limnology, Uppsala University, 752 36 Uppsala, Sweden
[3]Virginia Institute of Marine Science, College of William & Mary, Gloucester Pt., VA 23602, USA
[4]*Present address:* Swedish Meteorological and Hydrological Institute, 426 71 Västra Frölunda, Sweden
[5]*Present address:* CSIRO Oceans & Atmosphere, Hobart, Tasmania 7001, Australia
[6]*Present address:* School of Oceanography, Shanghai Jiao Tong University, Shanghai 200240, PR China

ABSTRACT: We assessed the distribution of biota (autotrophs and heterotrophs) and associated carbonate chemistry variables in Arctic sea ice at latitudes >82° N during late summer and early autumn 2018. The sampled sea ice was relatively thick (average 1.4 m) with variable snow cover (mean 7 cm) and low bulk salinities throughout. Most measured variables, including carbonate chemistry parameters, were low in the upper half of the ice cores, but increased with depth. Measurements of particulate organic carbon (POC), chlorophyll *a* (chl *a*), bacterial abundance, and particulate extracellular polysaccharide (pEPS) in the cores strongly suggested that detrital carbon was the major particulate organic pool. Near the ice–water interface, autotrophic material comprised ca. 50% of the total POC, whereas pEPS and bacterial carbon accounted for ca. 8 and 1% of the total POC, respectively. Under-ice water was nutrient poor, providing only a small input of nutrients to support autotrophic growth, at least during the time of our sampling. While the Arctic Ocean has substantial interannual variability in sea-ice concentration and thickness, these measurements enrich the available database and suggest that during years when autumn sea ice is >1 m thick, sea-ice biota are limited in activity and biomass.

KEY WORDS: Algae · Bacteria · Sea ice microbial community · Carbon · Biomass · EPS · DIC · pH

1. INTRODUCTION

Sea-ice cover is a central variable to polar oceanography and ecology. Arctic sea-ice extent has decreased by 13% per decade since 1981 (Thompson 2021), with summer declines of ca. 40% since 1981. Furthermore, the mean thickness of sea ice has been decreasing by 15% per decade (Comiso 2010), and total volume of ice has decreased by over 50% since 1981 (Kwok & Cunningham 2015). In addition, substantial interannual variability in ice distribution and thickness occurs. For example, in the past decade sea ice concentration at the North Pole has been greatly reduced during some summers, while in other years the ice concentration exceeded 98% (Belter et al. 2021). Sea ice in polar systems supports an active biological community that exchanges with oceanic water and is influenced by atmospheric processes (Deming & Collins 2017). The biota includes primary producers (often diatoms), heterotrophic prokaryotes and eukaryotes, and more mobile organisms (e.g. meiofauna, amphipods, small fish) that use the sym-

*Corresponding author: andtor@uw.edu

pagic biota as a food source (Kohlbach et al. 2016, Kohlbach et al. 2017). As sea ice melts in the summer, ice biota are released into the water column. With a greatly reduced ice cover, the magnitude of the release of ice communities and their impacts on the water columns across the Arctic are also greatly diminished (Fernández-Méndez et al. 2015), although there is uncertainty about the magnitude and phenology of the effects (Tedesco et al. 2019).

The Arctic Ocean is changing rapidly as a result of anthropogenic changes in the global environment, as increased concentrations of atmospheric carbon dioxide (CO_2) and other greenhouse gases have changed the heat balance of the region, which in turn has altered sea-ice thickness and extent (e.g. Kashiwase et al. 2017). As a direct result of atmospheric CO_2 uptake by the ocean, the pH of surface waters has decreased measurably (e.g. Doney et al. 2009); furthermore, changes in the ocean's surface carbonate chemistry are expected to continue in the future, including continued reduced pH levels and increased CO_2 concentrations. Environmental changes such as temperature increases can have extensive biological impacts at all trophic levels in the Arctic (changes in growth rates, modifications of currents, altered phenology; Tedesco et al. 2019), but these effects have not been fully assessed in high-latitude Arctic regions or on Arctic sea-ice biota.

Understanding the role of sea-ice microbial processes at high latitudes in the Arctic Ocean is central to a complete assessment of the ocean's response to climate change (Lund-Hansen et al. 2015, Cimoli et al. 2017), yet characterization of ice biota and the ice environment remains challenging due to the logistical constraints of sampling sea ice and the lack of large-scale remote sensing methods capable of assessing biological processes across extensive ice-covered areas. Changes in water-column biomass, driven in part by changes in sea-ice and snow concentrations and by increased nutrient loading from rivers (Fernández-Méndez et al. 2015, Lewis et al. 2020, Terhaar et al. 2021), can lead to alterations of sea-ice biomass. Novel methods for measuring ice algal biomass and growth have been initiated (Lange et al. 2017, Castellani et al. 2020, Torstensson et al. 2021), but strong spatio-temporal variability limits an ability to assess the role of sea-ice algal biomass.

Expeditions to the central Arctic (north of 82° N) remain challenging due to ice concentrations, cost, and limited ship availability. Despite these challenges, a number of research cruises have collected oceanographic data in the central Arctic in the past 3 decades (e.g. Tucker et al. 1999, Childers & Brozena 2005, Ross et al. 2021, Snoeijs-Leijonmalm et al. 2021), but relatively few included investigations of sea-ice characteristics and biota. For example, Bowman et al. (2012) reported on sea-ice microbial community structure in multi-year ice cores north of 88° N, and Lund-Hansen et al. (2015) investigated algal parameters in bottom sea ice at stations north of 82° N in late summer (31 July – 14 September 2012), including a number of stations located near the North Pole. At their stations north of 86° N, where the majority of the samples used in the present study were collected (Table S1 in the Supplement at www.int-res.com/articles/suppl/m703p017_supp.pdf), chlorophyll concentrations in the water under the ice averaged 0.17 µg l^{-1}, and ice chlorophyll levels averaged 0.11 mg m^{-2} in cores 126–272 cm thick.

In late summer 2018, we conducted measurements of the physical, chemical, and biological components of sea ice of the Arctic along the path of an icebreaker from the ice edge at 82° N to the North Pole, which was completely covered by ice (near 100% ice concentration). We hypothesized that in the central Arctic at this time of year environmental and biological conditions, both within the ice and in seawater directly under the ice, would be homogeneously distributed across broad scales. We further hypothesized that ice–seawater exchanges would strongly influence the vertical structure of biota and environmental variables within the ice. Along with snow cover, ice thickness, temperature, and bulk salinity, we measured the carbonate chemistry and microbial components (both auto- and heterotrophic) within multiple sections of 27 ice cores and in the water directly under the ice. We aimed to provide a basis for evaluating contemporary distributions of these sea-ice properties and to enable future investigators to compare data and quantify the impacts of continuing changes in the central Arctic Ocean. Our earlier work from the same expedition (Torstensson et al. 2021) reported on the largely negligible effects of elevated CO_2 on growth and development of ice biota, while here we considerably expand the available data on vertical distributions of chemical and biological properties in late-summer central Arctic sea ice with a view towards assessing future changes.

2. MATERIALS AND METHODS

2.1. Ice core sampling

Sea ice was sampled at 27 stations at various locations in the Arctic, between 82 and 90° N, during an

expedition on the RVIB 'Oden' from 5 August to 18 September 2018 (Fig. 1; Table S1). Most of the ice sampling was conducted away from the ship after transport of personnel from the ship to the sampling sites by helicopter. The ship was moored to a large ice floe from 14 August to 14 September (drifting between 88 and 89° N, so that the spatial coverage of ice stations was restricted. Remote sampling locations were chosen based on floe size, regularity of surface topography, and distance from the ship. All ice sampled had persisted through summer, remaining by early autumn. Although the precise age of the ice was not determined, estimates were made based on sampling season, ice thickness, and bulk salinity profiles. The atmospheric temperature and depth of snow cover were measured immediately upon selection of the sampling site. Ice cores were taken using a battery-driven 9 cm diameter Kovacs ice corer. All cores were collected within an area of 6 m^2, generally at a distance of 50 cm from each other, to minimize the impacts of spatial variability within the ice floe. Coefficients of variation of chlorophyll *a* (chl *a*) concentration in bottom ice core sections were derived from a different study, measured at 4 of the stations, and was on average (±SD) 17.7 ± 5% (n = 4, Torstensson et al. 2021). The depth of the ice was measured once the core was removed using a Kovacs ice thickness gauge. Once collected, the core was placed in a wooden cradle where its total length was measured. Ice temperatures were measured in the first ice core at 10 cm intervals from the center of the core after a small hole was drilled, into which a digital thermistor (Amadigit; accuracy of 0.1°C) was inserted and the temperature recorded. The first ice core was sectioned in 10 cm intervals using a using a custom alloy bow saw immediately after temperature was recorded and placed in gas-impermeable Tedlar® bags. The atmosphere was evacuated from the bags immediately after sample collection (Granfors et al. 2013). Following melt in the dark at room temperature, dissolved inorganic carbon (DIC) concentrations, pH, and bulk salinity of the sample were measured. Bulk salinity was measured using a con-

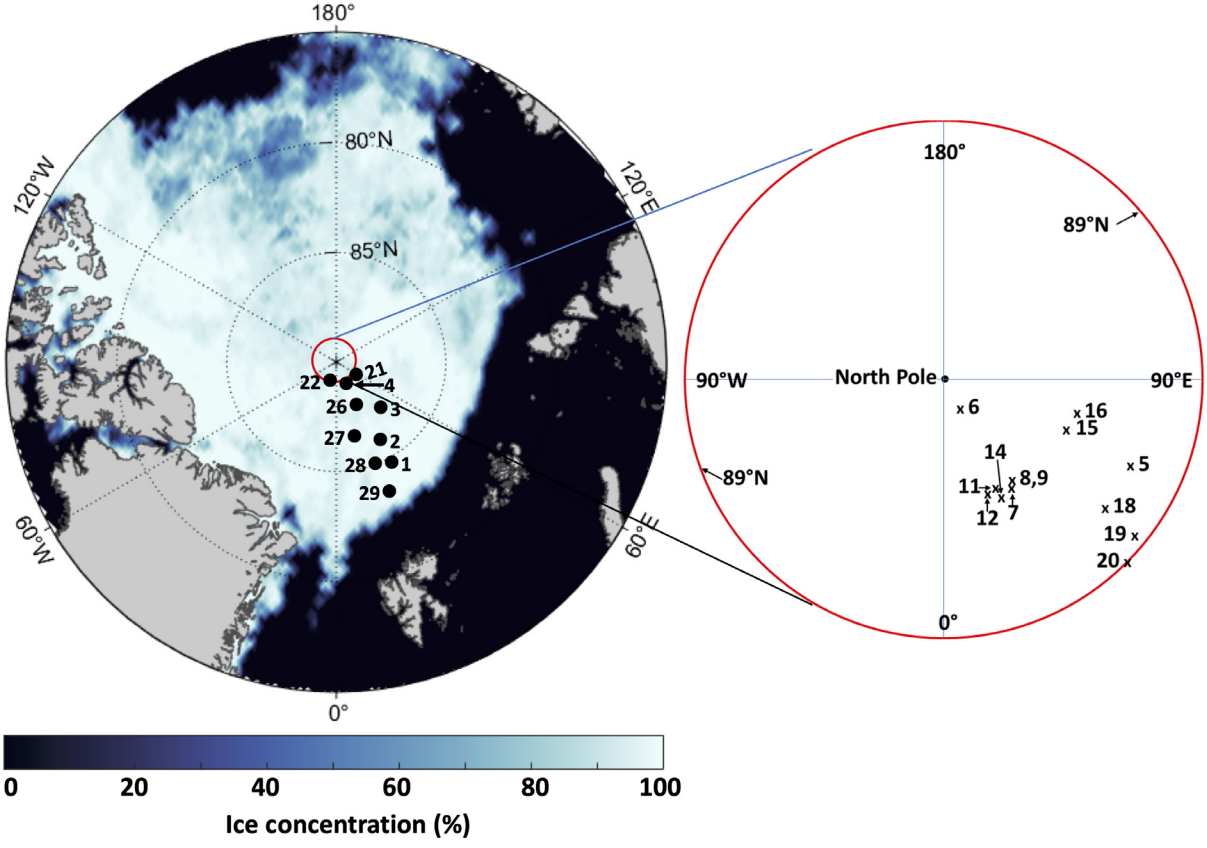

Fig. 1. Sea-ice distribution in the Arctic Ocean on 1 September 2018 and the locations where ice cores were collected. Insert shows the locations of the large number of stations close to the North Pole. Sea-ice concentration was obtained using Advanced Microwave Scanning Radiometer 2 (AMSR2) at 3.125 km resolution on 12 August 2018 and processed with the ASI algorithm, version 5.4 (Spreen et al. 2008)

ductivity meter (WTW Cond 330i) with a precision and accuracy of ±0.5%. Brine volume and brine salinity were calculated from bulk salinity and ice temperature according to Cox & Weeks (1983) and Leppäranta & Manninen (1988). Sections (10 cm, starting from the top) of additional cores were sampled for biological and other chemical measurements, and placed in Whirl-Pak® bags. All bagged sections were stored in a darkened cooler while on site.

Due to the volume of samples to be melted and processed, core sections occasionally were taken only at the top, middle and bottom of each core. We recognize that substantial variability can occur in sea ice on smaller spatial scales, as shown for the expedition by Torstensson et al. (2021), but we did not address the causes of such variations in the present study. Visual observations from a remotely operated vehicle suggested that larger-scale variability was minimal in areas that were relatively uniform in ice thickness and topography (Anhaus et al. 2021). Multiple ice thickness and snow cover measurements were always similar within one station (within ~5 and 1 cm of each other, respectively). All sectioned cores were returned to the ship for further processing and analyses. Data were assessed both on an absolute scale of depth as well as relative to the bottom depth to determine the extent of the influence of seawater on core properties.

In the laboratory onboard the ship, core sections had 1.0 l of cold (−1.6°C), filtered (through 0.2 µm Pall PES filters) seawater (from ca. 1000 m depth) added to each Whirl-Pak® bag and placed in the dark at ca. 15°C for melting. Seawater was added to reduce the likelihood of osmotic disruption of cells; deep seawater was used primarily to ensure a constant salinity background for the melting process, while also avoiding additions that would influence subsequent measurements. Upon complete ice melt (from 12 to 24 h), the total volume of the melt and filtered seawater mixture was recorded, and subsamples were taken for bacterial abundance and concentrations of particulate extracellular polysaccharides (pEPS), chl *a*, and particulate organic carbon (POC) and nitrogen (PON). All values were corrected for seawater dilution.

Water directly under the ice floe was collected for biological and nutrient measurements using a hand-operated pump. After the cores were collected and processed, we lowered a rubber tube down the bore hole into the water. Seawater was pumped to the surface and collected in 1 l polycarbonate bottles, which were then placed in the dark. Temperatures of the below-ice water samples were recorded immediately. Upon return to the onboard laboratory, samples for nutrients, chl *a*, POC, PON, pEPS, salinity, DIC, and pH were processed as for ice-core samples.

2.2. Chemical analyses

The DIC concentrations were measured using an automated infra-red inorganic carbon analyzer (AIRICA) coupled with a LI-COR LI-7000 CO_2/H_2O analyzer, having a manufacturer precision of 1.5 µmol kg^{-1} (Torstensson et al. 2021). A certified reference material (CRM; provided by Andrew G. Dickson, Scripps Institution of Oceanography, CA, USA) was analyzed to establish a 'conversion factor' that was applied so that the following CRMs were within 2 µmol kg^{-1} of the certified concentration. All inorganic carbon measurements were conducted on the same ice core, and details of the methodology are provided by Torstensson et al. (2021). Analysis of DIC was always conducted first, followed by pH and salinity measurements. Following measurement of DIC and pH on a total scale (pH_T), total alkalinity (TA), and pCO_2 were computed using the $CO2_{sys}$ program of van Heuven et al. (2011), using the carbonic acid dissociation constants of Roy et al. (1993). In the absence of phosphate and silicate measurements, we used null values for these 2 nutrients in the carbonate system computations. While this approach introduces uncertainty to the computed parameters, the uncertainty is much smaller than the standard deviation of the computed parameters. Filtered samples for seawater nutrients (ca. 40 ml) were stored frozen in sterile 50 ml plastic tubes and analyzed using a QuAAtro autoanalyzer at the University of Gothenburg, Sweden, upon completion of the cruise.

2.3. Biological samples

Chl *a* was quantified using standard fluorometric techniques using the non-acidification method (Welschmeyer 1994). The fluorometer was calibrated prior to the cruise using commercially purified chl *a* (Sigma). POC and PON samples were collected by filtering known volumes through precombusted (450°C for 2 h) Whatman GFF filters (25 mm), rinsed with 5 ml of weak acid (0.01N HCl in cold filtered seawater), stored in combusted glass vials covered with combusted aluminum foil, and dried at 60°C. Blanks were filters through which 3 ml of 0.2 µm fil-

tered seawater were passed. Samples were oxidized on a Costech ECS Model 4010 elemental analyzer using an acetanilide standard (Gardner et al. 2000).

Particulate extracellular polysaccharide samples were collected on 0.4 µm Nucleopore filters and analyzed using the phenol-sulfuric acid assay (DuBois et al. 1956). This analysis provides results in glucose equivalents, which we converted into carbon units using a conversion factor of 33.3 (Cooper et al. 2019). Samples for bacterial abundance were fixed in 2% formaldehyde and stored at −20°C until further processing. Free and particle-attached bacterial cells were counted by epifluorescence microscopy, using the dual staining technique with 4′-6′-diamidino-2-phenylindole (DAPI) and *N,N,N′,N′*-tetramethylacridine-3,6-diamine (acridine orange), following Kuwae & Hosokawa (1999). Bacterial biomass was estimated by converting abundance into biomass by assuming 20 fg C cell^{-1} (Lee & Fuhrman 1987).

3. RESULTS

Hourly air temperatures measured from the onboard meteorological tower ranged between −6.7 and 0.6°C (mean of −1.2°C) and between −14.7 and −0.8°C (mean of −5.9°C) during the sampling period in August and September, respectively (Table S1). Sea-ice thickness ranged between 74 and 177 cm (mean 141.8 cm, n = 24), with a snow cover of 2 to 7 cm (mean 4.8 cm, n = 20). Sea-ice temperatures ranged from −3.2 to 0.0°C (Table 1, Fig. 2); the warmest temperatures were recorded in the upper ice in locations sampled close to the southern ice edge during the north-bound transect (Fig. 1), although stations in similar locations sampled 40 d later were substantially colder (by ca. 2.5°C). No spatial pattern in temperature was observed. Mean temperatures were lowest in the bottom of the cores (−1.64°C) and highest 25 cm under the snow cover (−0.50°C; Fig. 2). Significant freshening was observed in the upper ice core sections, and the entire ice cores were largely characterized by low bulk salinities (all values <5.4; Fig. 2) and high brine volume fractions (>0.05; Fig. 3). Ice-core bulk salinities exhibited a strong vertical gradient in the upper half of the cores, followed by a more isohaline distribution in the bottom half (Fig. 2). Salinity in the upper 25% of the cores ranged from 0 to 2.3, and from 1.3 to 5.3 in the lower 25% of the cores (Table 1). Temperature and salinity profiles for individual stations are provided in Figs. S1 & S2, and station-averaged data for all parameters are provided in Tables S2 & S3. No relationship between core-averaged bulk salinity and ice thickness was observed (linear regression; $R^2 = 0.044$, $p > 0.05$).

Carbonate system parameters in the ice also varied in a manner similar to bulk salinity and temperature. DIC concentrations were low in the upper 30 cm, increased with depth, and became relatively constant within the bottom 30% of the ice cores (Fig. 4, Table 2). Total alkalinity and pH showed similar patterns (Table 2). Maximum pH values, near 8.5, were observed in the lower portion of the cores. The mean DIC concentration in the lower 10 cm of the cores was 189 µmol kg^{-1} (Table 2). Ratios of TA:DIC were highest in the bottom layers of the cores (averaging 0.86, 1.06, and 1.15 in the top, middle, and bottom layers, respectively; Table 2).

The distribution of biological material in the sea ice also showed strong vertical gradients. All ice cores had the greatest amount of chl *a* in the bottom 10 cm section and declined steeply above the bottom horizon (Fig. 5). Mean chl *a* concentration in the bottom section of the cores was 8.71 µg l^{-1} (Table 3). POC gradients were generally less steep, ranging from 23.0 to 72.3 µmol l^{-1} from top to bottom. On average, 46% of the chl *a* and 14.6% of the POC were located in the bottom section (Fig. 5). Bacterial abundance generally followed the distribution of chl *a*, although a smaller fraction of the standing stock of bacteria was concentrated near the center of the ice core compared to the surface and bottom sections (Table 3). Neither bacterial abundance nor biomass estimates correlated with chl *a* concentration (n = 25, R^2 = 0.038, p = 0.176), suggesting that the relationship

Table 1. Means ± SD, ranges, and numbers of samples (n) of top, middle, and bottom sections of sea-ice cores for temperature and bulk salinity

Core section		Section depth (cm)	Temperature (°C)	Salinity
Top	Mean	6.8 ± 3.8	−0.82 ± 1.01	0.66 ± 0.71
	Range	5–15	−3.13 to 0.01	0.00–2.10
	n	24	32	32
Middle	Mean	71.8 ± 18.0	−0.86 ± 0.37	2.49 ± 1.11
	Range	32.5–112.5	−1.67 to −0.30	1.4–4.5
	n	35	22	22
Bottom	Mean	137.3 ± 28.1	−1.48 ± 0.19	2.99 ± 0.87
	Range	73–175	−1.10 to −1.78	1.4–4.5
	n	24	23	23

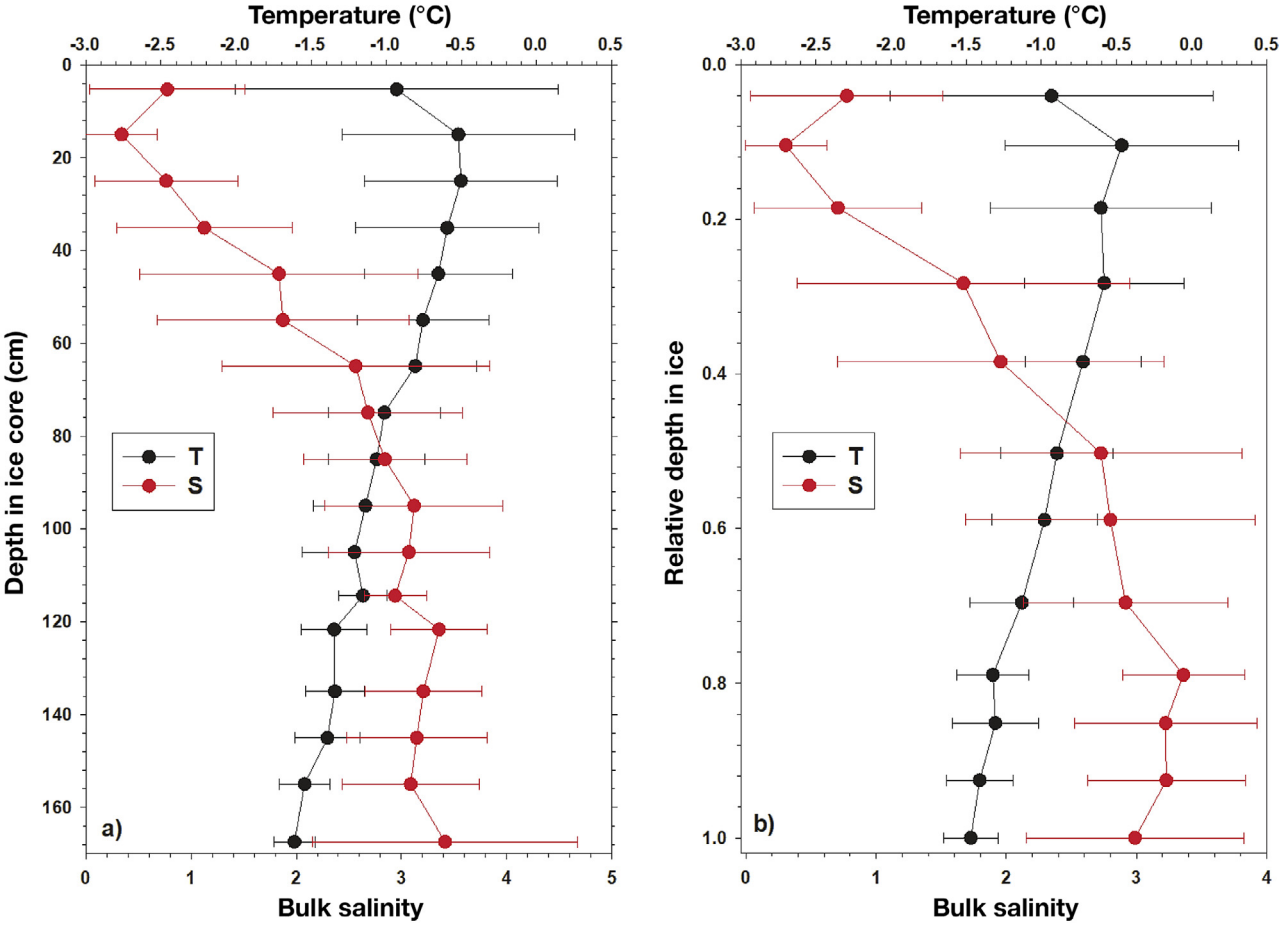

Fig. 2. Mean vertical distribution of temperature (T) and bulk salinity (S) within the sea-ice cores, expressed as (a) mid-points of each core section and (b) percentage of the total core depth. Error bars represent SD (n = 24)

between autotrophs and heterotrophs was weak or indirect. Estimates of the contribution of bacteria to total POC ranged from 0.57 to 1.01%, indicating a minor contribution of bacterial biomass to the total organic load (Table 3). In contrast, phytoplankton accounted for 5.9 to 39% of the POC, with greatest contributions in the lower portions of cores. pEPS contributed from 7.7 to 8.9% of the POC (Table 3). Ratios of POC:chl *a* were very high in the surface of ice cores, and decreased with proximity to seawater (Fig. 6). Similarly, POC:PON ratios were high near the ice–snow interface, and decreased with depth. POC:PON ratios were significantly higher in the bottom sea ice compared to the under-ice water (14.5 and 7.0, respectively, $p < 0.001$, *t*-test).

To assess if there was a temporal pattern in ice biota that was independent of location, we integrated chl *a* and POC concentrations and investigated these values based on time of sampling (Fig. 7). Integrated concentrations ranged from 0.03 to 1.13 mg m^{-2} and 1.26 to 14.9 mmol C m^{-2} for chl *a* and POC, respectively (Fig. 7). There was no obvious temporal pattern in organic matter, suggesting that spatial differences were the more important variable in the distributions of biota. However, as with temperature, there was no correlation between biological variables and distance to the ice edge (linear regressions, $p > 0.05$), indicating that spatial variability on a smaller scale was the dominant scale contributing to the patterns we observed. There was no significant correlation between integrated POC concentration and snow depth (linear regression, $p = 0.34$).

Nutrient concentrations in the underlying water were low. Mean ± SD (n = 15) $NO_2 + NO_3$, NH_4, PO_4, and $Si(OH)_4$ concentrations in the under-ice water were 1.8 ± 0.7, 0.8 ± 0.3, 0.67 ± 0.2 and 4.6 ± 0.3 µM, respectively (Table 4), suggesting a substantial uptake of nutrients by phytoplankton during the movement of the water mass from the North Atlantic into the central Arctic (e.g. Randelhoff et al. 2020). There were no significant correlations between inorganic nutrient concentrations ($NO_2 + NO_3$, PO_4, and $Si(OH)_4$) in the underlying water and POC concentration in the bottom sea ice (linear regressions, $p > 0.27$).

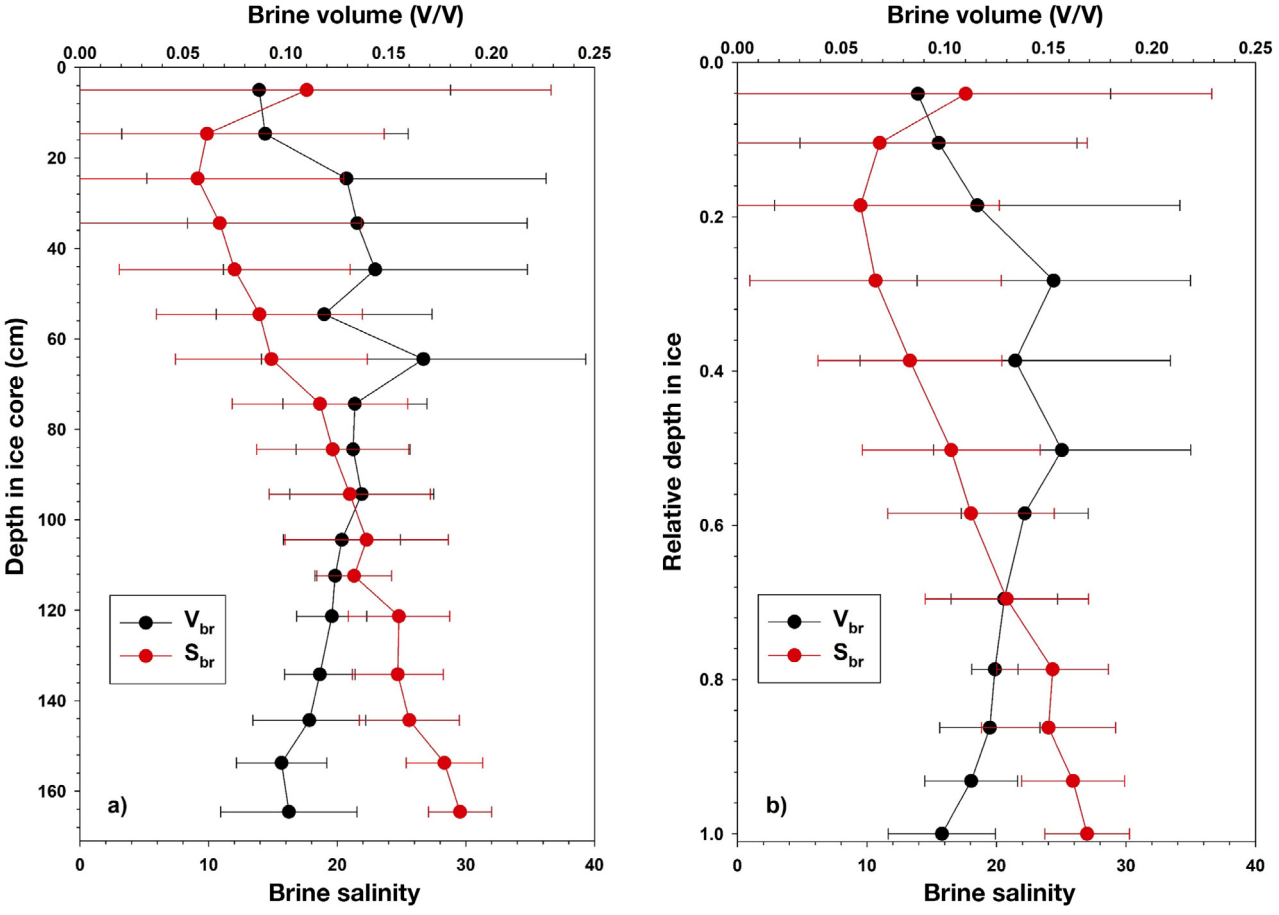

Fig. 3. Mean vertical distribution of brine volume fraction (V_{br}) and brine bulk salinity (S_{br}) within the sea-ice cores, calculated according to Cox & Weeks (1983) and Leppäranta & Manninen (1988), and expressed as (a) mid-points of each core section and (b) percentage of the total core depth. Error bars represent SD (n = 24)

4. DISCUSSION

Given the importance of sea ice and its associated biota to the Arctic system (Fernández-Méndez et al. 2015, Arrigo 2017) and the rapidly changing environmental conditions occurring in the central Arctic Ocean, the effects of these changes on the biology and carbonate chemistry of the ice need to be understood and included in predictions of continued anthropogenic forcing. Environmental monitoring of sea-ice microbial communities is a critical task in the understanding of the consequences of a reduced sea-ice cover, yet the available data from pack ice in the central Arctic is limited. Our study presents a unique combination of concurrent observations of carbonate chemistry and concentrations of chl *a*, bacteria, pEPS, POC, and PON in late-summer central Arctic sea ice; our results, which for each variable fall within the range of values reported in earlier studies of the central Arctic (Gosselin et al. 1997, Gradinger 1999, Bowman et al. 2012, Fernández-Méndez et al. 2015, Lund-Hansen et al. 2015, Castellani et al. 2020), considerably enrich the available data.

Multiyear sea ice has low bulk salinities compared to first-year ice, as summer surface meltwater can repeatedly flush salts downward and out of the sea-ice matrix (e.g. Notz & Worster 2009). Our observations of ice near the North Pole and other sampling sites displayed very low bulk salinities throughout the cores (Fig. 2). While we have no measurement of the precise age of our sampled ice floes, the consistently observed low salinities strongly suggest that the floes were 1–3 yr old. Furthermore, as the ice floes had persisted through summer, remaining in early autumn, and were up to 2 m in thickness, most ice floes sampled were likely 1–2 yr old, which is also supported by comparing individual salinity profiles to the sea-ice age classification description of Warner et al. (2013).

Relatively few observations of carbonate chemistry parameters have been made in Arctic sea ice (Søgaard et al. 2013), and to our knowledge, none from

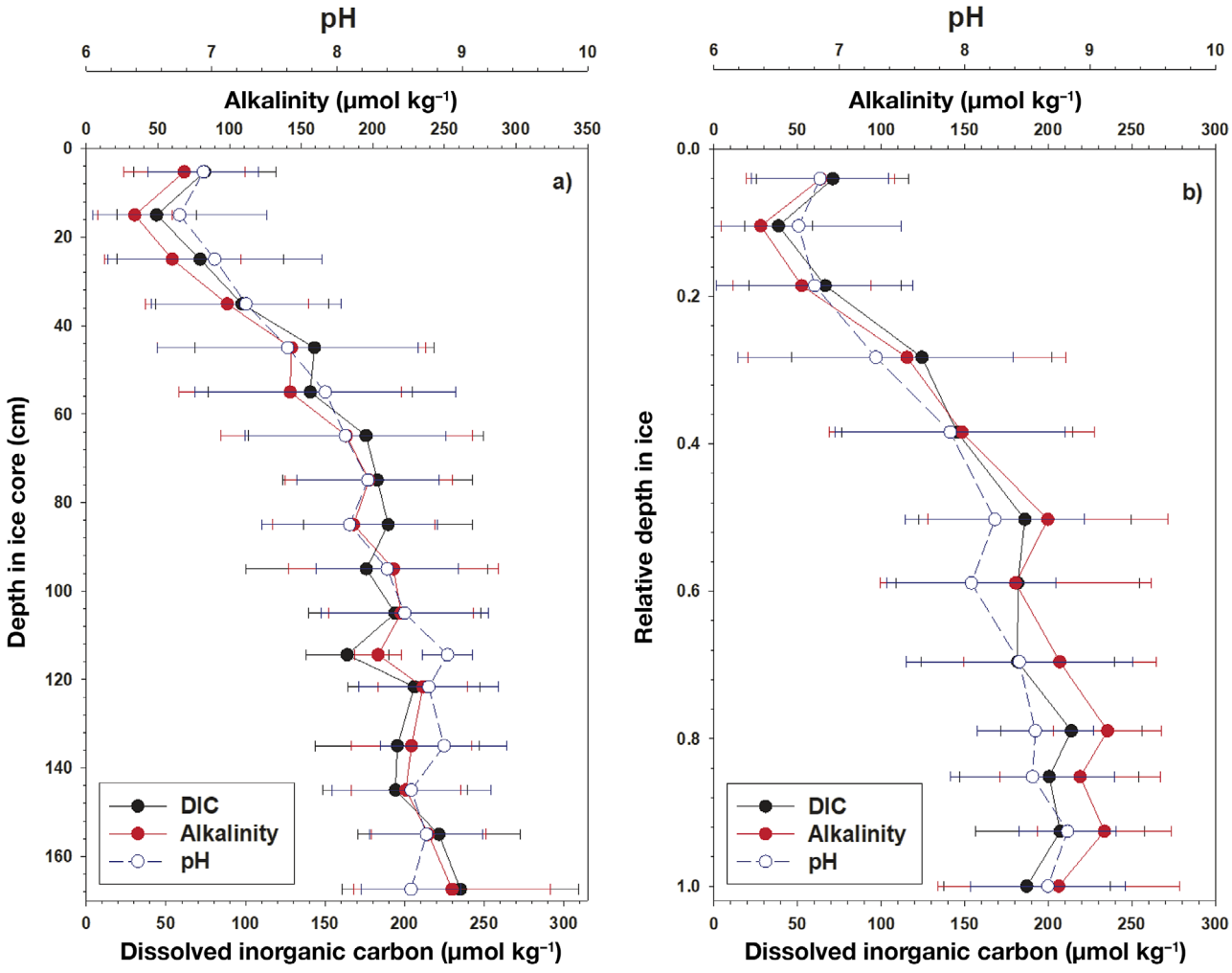

Fig. 4. Mean vertical distribution of dissolved inorganic carbon (DIC), alkalinity, and pH within the sea-ice cores, expressed as (a) mid-points of each core section and (b) percentage of the total core depth. Error bars represent SD (n = 17)

Table 2. Mean ± SD, range, and numbers of samples (n) of top, middle, and bottom sections of sea-ice cores for dissolved inorganic carbon concentration (DIC), alkalinity, pH and pCO_2 concentration, with DIC:alkalinity ratios calculated from the means

Core section		DIC (µmol kg^{-1})	Alkalinity (µmol kg^{-1})	DIC:alkalinity ratio	pH	pCO_2 (matm)
Top	Mean	66.2 ± 42.9	57.0 ± 43.3	0.86	6.79 ± 0.54	197 ± 163
	Range	14.5–156	0.30–146		5.60–7.69	32.3–740
	n	23	23		18	18
Middle	Mean	171 ± 67.8	181 ± 79.4	1.06	8.16 ± 0.73	74.1 ± 116
	Range	77.1–339	56.6–373		6.72–9.21	1.87–403
	n	23	21		21	21
Bottom	Mean	189 ± 51.7	216 ± 55.2	1.15	8.66 ± 0.62	29.4 ± 56.2
	Range	88.0–294	88.0–314		7.26–9.40	0.96–217
	n	21	20		20	20

the central Arctic except our own from this same expedition, reported by Torstensson et al. (2021). Our observations indicate DIC concentrations that are consistent with the lower bulk salinities in the measured cores and that are lower than earlier work in the Canadian Arctic Archipelago (Geilfus et al. 2012, Fransson et al. 2013). The TA:DIC ratios reported here (0.91–1.45) for lower ice sections are consistent

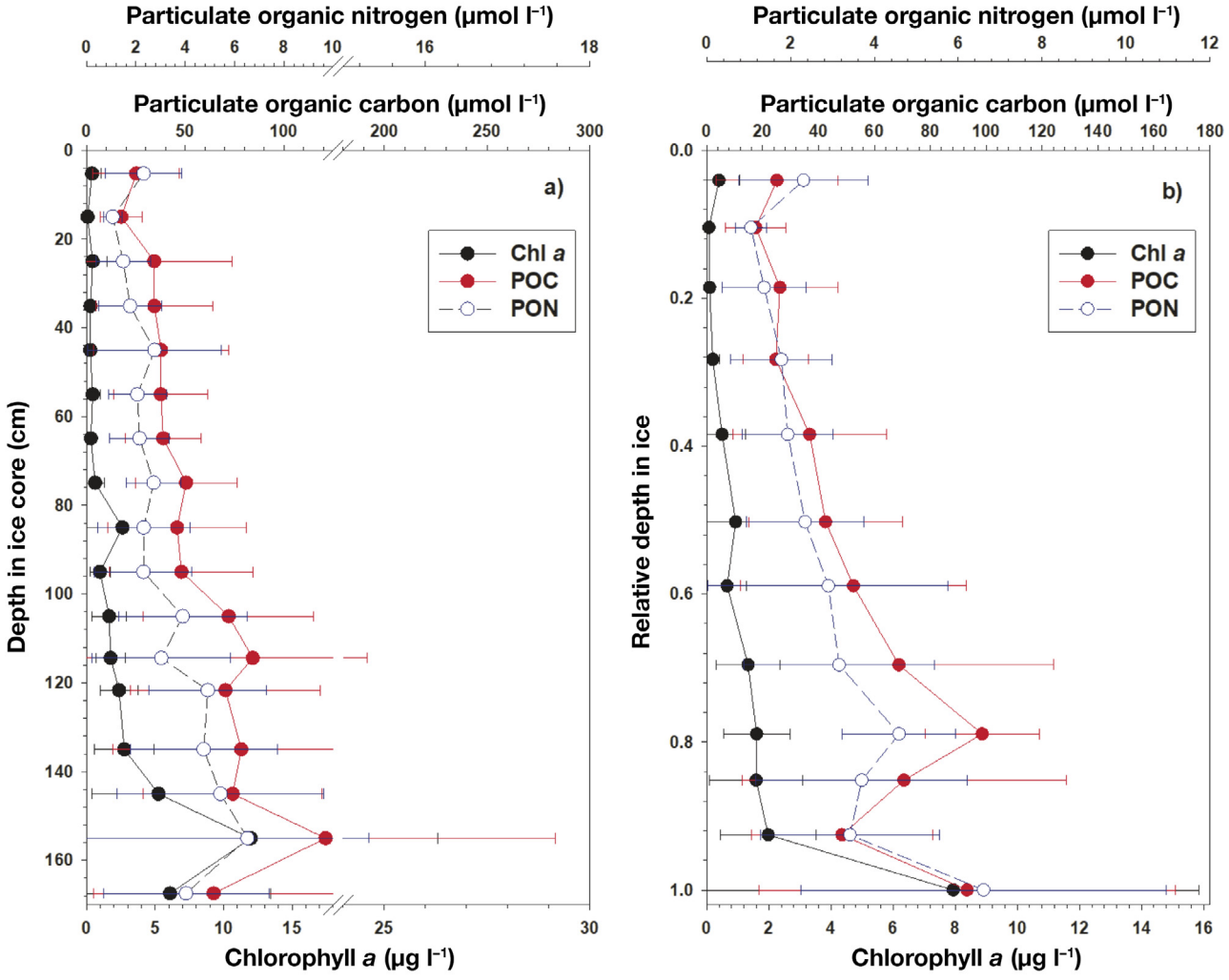

Fig. 5. Mean vertical distribution of chlorophyll *a* (chl *a*), particulate organic carbon (POC), and particulate organic nitrogen (PON) within the sea-ice cores, expressed as (a) mid-points of each core section and (b) percentage of the total core depth. Error bars represent SD (n = 17)

Table 3. Means ± SD, ranges, and numbers of samples (n) of top, middle, and bottom sections of sea-ice cores for concentrations of chlorophyll *a* (chl *a*), particulate organic carbon (POC), particulate organic nitrogen (PON), and particulate extracellular polysaccharide (pEPS), and bacterial abundance, including estimates of proportional contributions to POC

Core section		Chl a (µg l^{-1})	POC (µmol l^{-1})	PON (µmol l^{-1})	pEPS (µmol C l^{-1})	Bacterial abundance (× 10^3 ml^{-1})	Algal portion of POC (%)	pEPS portionof POC (%)	Bacterial portion of POC (%)
Top	Mean	0.18 ± 0.24	23.3 ± 20.1	2.09 ± 1.45	2.08 ± 1.16	76.3 ± 62.2	5.87	8.94	0.05
	Range	0.01–0.86	1.53–73.1	0.44–5.31	0.56–4.47	10.5–159			
	n	14	11	10	13	4			
Middle	Mean	1.18 ± 2.26	51.7 ± 35.8	2.93 ± 2.36	4.56 ± 2.88	509 ± 551	8.43	8.87	0.12
	Range	0.11–9.37	4.45–131	0.37–9.80	1.68–11.8	40.5–1810			
	n	16	13	14	16	15			
Bottom	Mean	8.71 ± 8.20	88.5 ± 78.1	6.55 ± 4.51	6.85 ± 5.07	537 ± 291	39.2	7.74	0.08
	Range	0.16–30.9	5.47–307	1.34–16.7	1.92–19.7	37.3–1180			
	n	14	14	14	15	13			

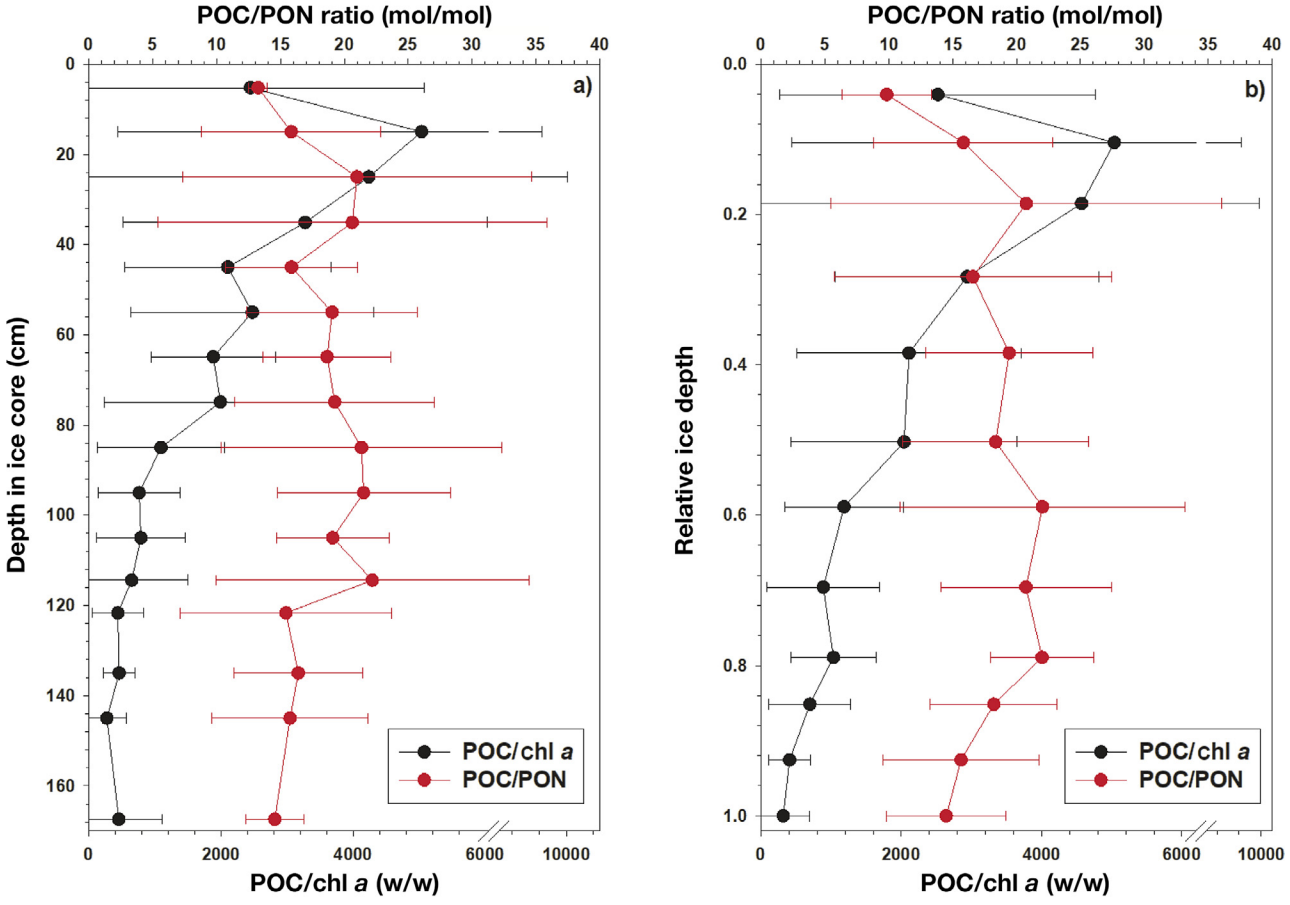

Fig. 6. Mean vertical distribution of the POC:PON and POC:chl *a* ratios within ice cores, expressed as (a) mid-points of each core section and (b) percentage of the total core depth. Error bars represent SD (n = 17)

with earlier estimates from coastal Arctic and sub-Arctic sea ice (0.9–2.2, Rysgaard et al. 2007; average of 1.25, Søgaard et al. 2013), but in the upper sections we found values <1.0.

The exceptionally elevated POC:chl *a* ratios we observed (from 200 to 5000; Fig. 6) suggest a substantial contribution of detritus to the POC concentrations. In addition to these high ratios, POC:PON ratios in sea ice were high compared to the under-ice water (14.5 in the bottom section vs. 7.0 in surface seawater), further suggesting that the contribution of detritus in ice to the POC pool was large. The POC:PON and POC:chl *a* ratios were generally lower in the bottom sections of the ice (although still very high relative to actively growing phytoplankton), indicating that the autotrophic activity and biomass in the lower sections were slightly greater than in the upper portions of the cores. The mean POC:chl *a* level in the bottom segments was 206 (w/w), whereas actively growing phytoplankton have ratios from 30 to 50 when grown with sufficient nutrients and saturating irradiances (Geider et al. 1998). As autotrophs do increase their POC:chl *a* ratios under nutrient limitation, the effects of low nutrients may have contributed to the increased ratios observed. However, during our study (August–September), nitrate concentrations were sufficiently low in the under-ice water to limit phytoplankton growth (Mills et al. 2018). No nutrient data from the sea ice are available from our study, but given the temperatures and brine volume fractions of the sea ice, fluid permeability would have been high. We therefore expect the sea-ice microorganisms, predominantly located in the bottom of the ice, to have experienced a chemical environment similar to that found in the under-ice water. In support of this expectation, parallel incubation experiments with sea-ice sections placed in nutrient-rich seawater collected at 200 m resulted in significantly stimulated microbial growth, although elevated CO_2 levels did not affect the growth of the microorganisms or the composition of bacterial species (Torstensson et al. 2021).

Analysis of pEPS and bacterial abundance indicate that approximately 8% of the total POC consisted of

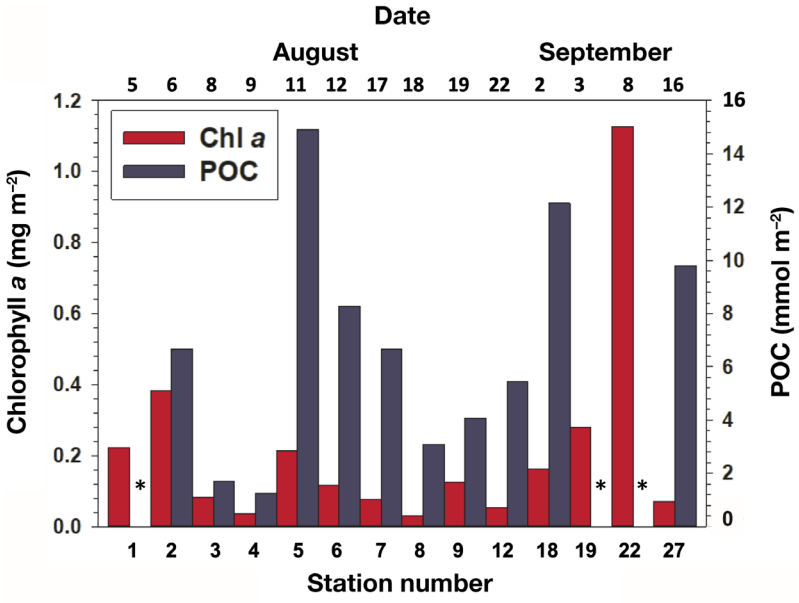

Fig. 7. Depth-integrated chlorophyll *a* (chl *a*) and particulate organic carbon (POC) within sea-ice cores as a function of station number (which reflects the time sampled). Asterisks indicate no data. Full-depth profiles were completed at all stations except Stns 1, 2, 19, and 22

polysaccharide substances, and only a small fraction was contributed by bacteria (<1%; Table 3). However, sea-ice bacteria can be larger in size compared to the bacterioplankton used in the cell-to-carbon conversion applied in our study (Lee & Fuhrman 1987, Gradinger & Zhang 1997), which may have resulted in an underestimation of the bacterial contribution to POC. However, even if the conversion factor were 5-fold higher, bacterial contribution to POC would remain at less than 1%. The contribution of EPS to the total organic carbon pool may also be underestimated, as not all pEPS may be retained during filtration through the GFF filters used for POC measurements. Furthermore, the conversion of EPS levels to carbon units involves some uncertainty as the composition of pEPS is complex. A recent study identified carbohydrate-rich EPS to be a significant contribution to the organic matter concentrations in late summer sea ice in the Arctic Ocean, and reported that bacterial activity strongly correlated with carbohydrate concentration, but not with bacterial biomass (Piontek et al. 2021). Therefore, arguably, rates of microbial activities that affect biogeochemical processes (e.g. CO_2 uptake and release) may be de-coupled from the algal and bacterial standing stocks presented in our study. As previously suggested, bacterial and algal turnover of

Table 4. Chemical and biological characteristics of under-ice water. N+N: nitrate plus nitrite; NH_4: ammonium; PO_4: phosphate; $Si(OH)_4$: silicic acid; Chl *a*: chlorophyll *a*; POC: particulate organic carbon; PON: particulate organic nitrogen; pEPS: particulate extracellular polysaccharide; ND: no data; ROV: remotely operated vehicle

Station number	Salinity	N+N (µM)	NH_4 (µM)	PO_4 (µM)	$Si(OH)_4$ (µM)	Chl *a* (µg l^{-1})	POC (µmol l^{-1})	PON (µmol l^{-1})	pEPS (µmol C l^{-1})	Bacterial abundance ($\times 10^3$ ml^{-1})
3	ND	1.27	<0.20	1.02	7.05	ND	ND	ND	ND	324
4	24	2.48	<0.20	1.06	6.29	0.18	ND	ND	0.11	172
5	ND	1.43	<0.20	0.72	4.56	0.22	ND	ND	1.00	77
6	ND	1.32	<0.20	0.88	5.78	0.40	ND	ND	0.67	517
ROV	ND	ND	ND	ND	ND	1.25	7.28	1.20	ND	ND
8	ND	1.58	<0.20	0.74	5.94	0.87	8.91	1.53	1.00	171
9	ND	2.07	0.24	0.71	5.18	0.73	6.66	1.00	0.33	ND
11	ND	3.40	0.97	0.72	4.96	0.37	5.21	0.89	0.67	ND
12	ND	2.09	0.50	0.69	4.76	0.34	6.17	0.86	0.33	ND
16	ND	1.24	ND	0.68	4.61	0.50	ND	ND	ND	ND
18	ND	ND	ND	ND	ND	0.50	ND	ND	0.67	ND
19	30.9	ND	ND	ND	ND	0.36	ND	ND	0.33	ND
20	ND	ND	ND	ND	ND	0.52	ND	ND	ND	ND
21	ND	1.48	0.92	0.55	3.70	0.37	7.11	0.67	0.67	252
22	30.9	1.62	1.27	0.48	3.63	ND	ND	ND	0.67	266
25	ND	1.72	0.79	0.52	3.88	0.41	ND	ND	0.33	222
26	30.7	2.16	0.41	0.69	5.15	0.30	ND	ND	0.67	323
28	32.6	2.67	0.72	0.42	3.13	0.15	ND	ND	0.33	313
29	ND	0.95	1.09	0.20	0.44	0.44	ND	ND	0.67	278
Mean ± SD	29.8 ± 3.34	1.83 ± 0.65	0.76 ± 0.32	0.67 ± 0.22	4.60 ± 1.57	0.46 ± 0.27	6.89 ± 1.24	1.03 ± 0.30	0.56 ± 0.26	265 ± 113

nitrogen-containing compatible solutes may play an important role in nutrient cycling in the parts of sea ice that experience significant fluctuations in salinity, and could potentially continue to fuel primary production, even if nutrients are scarce in the surrounding seawater (Firth et al. 2016, Torstensson et al. 2019). Determining rates of bacterial activity are therefore key to identifying potential microbial hotspots for carbon biogeochemistry even in nutrient-depleted summer sea ice.

The sampled sea ice contained POC throughout the ice cores, which most likely originated from algal incorporation during the formation and growth of the ice, with subsequent growth and senescence of the algae and heterotrophic modification of the algal material. Given the amounts of POC in the ice relative to surface seawater (an average of 87 µmol l^{-1} in the bottom-ice section vs. 6.5 µmol l^{-1} in surface seawater), this carbon upon release may impact the local carbon budget and biogeochemical cycling. Released POC from melting sea ice, with its significant proportion of detrital carbon, can be expected to impact the Arctic biological pump and, depending on its fate in the upper water column, potentially the particulate flux to deep-sea communities (Boetius et al. 2013, Krumpen et al. 2019).

Integrated chl *a* values in our sea-ice cores indicate concentrations similar to those recorded in the central Arctic Ocean during the same period in 1991 and 1994 (Gosselin et al. 1997, Gradinger 1999), with values up to 14 mg chl *a* m^{-2} near 87.5° N but only ca. 1.2 mg chl *a* m^{-2} at 89° N. Our values ranged from 0.03 to 1.13 mg chl *a* m^{-2}, with the highest value occurring on 9 September at 88.7° N. Gradinger (1999) compiled data from 23 stations in the Arctic (all above 80° N) and reported a mean concentration of <1 mg chl *a* m^{-2} and maximum concentrations of ca. 7.5 mg chl *a* m^{-2}. Lund-Hansen et al. (2015) reported integrated chlorophyll levels from 0.01 to 0.52 mg chl *a* m^{-2}; Fernández-Méndez et al. (2015) found concentrations between 0.3 and 8 mg chl *a* m^{-2}. Although valuable, these relatively limited data on sea-ice chlorophyll levels in the central Arctic are insufficient to determine if a decline or increase has occurred in the past few decades; however, ice algal biomass will be impacted by decreasing thicknesses of ice and snow cover (Castellani et al. 2017, Lund-Hansen et al. 2020). Such changes would be strongly influenced not only by snow cover, which appears to be decreasing in the Arctic (Kwok et al. 2020), but also by nutrient inputs. Sea-ice chl *a* in the Pacific-influenced waters of the Arctic appears to be much greater than in those regions influenced by Atlantic inflow, with maximum pigment concentrations being 304 mg chl *a* m^{-2} (Gradinger 2009). This difference strongly suggests that nutrients play a significant role in promoting algal growth in sea ice (Mortenson et al. 2017, Dalman et al. 2019). Waters under the ice that we sampled were largely nutrient-poor (mean nitrate concentrations were <2 µM; Table 4); furthermore, long-term (over weeks) incubation of cores exposed to irradiances similar to their *in situ* levels but provided with elevated nutrients showed substantial growth and algal accumulation (Torstensson et al. 2021). While the irradiance levels under Arctic sea ice can be very low, sea-surface nutrients also have a substantial impact on determining the growth and accumulation of sea-ice algae (Castellani et al. 2017, Tedesco et al. 2019).

The low heterotrophic and autotrophic biomass we encountered in our sampling may represent one end of the spectrum of POC in sea ice, which varies because of ice thickness and age, snow cover, and influence of nutrient supply. By increasing the availability of systematic measurements from ice cores and underlying water, our data indicate that during years with high ice (>98%) concentrations, sea ice near the North Pole will likely support only a limited biotic assemblage in late summer–early autumn. Although there was a strong degree of water exchange between the sea ice and the under-ice seawater, as indicated by high brine volume fractions and temperatures, our data suggest that the nutrient exchange was not sufficient to support significant algal biomass in the ice during the study period. The data presented in this paper also provide baseline measurements for further work on the seasonal and interannual variability of sea-ice biota in the central Arctic (e.g. Nicolaus et al. 2022), which will undoubtedly increase our understanding of the processes occurring in ice floes and their importance to the carbon budget in both the ice and the water column.

Acknowledgements. This research was part of the Arctic Ocean (AO) 2018 expedition conducted during the 'Oden' Arctic Ocean 2018 (AO2018) Cruise and was funded by the US National Science Foundation (Grants 1734786 and 1734947) and the Swedish Research Council (2017-06205). The Swedish Polar Research Secretariat (SPRS) provided access to the icebreaker 'Oden' and logistical support. We are grateful to the SPRS logistical staff, to Captain Mattias Peterson and his crew, and to the helicopter crew of Sven Stenvall and Magnus Holmén for their assistance in the many phases of the project. We also thank Katarina Abrahamsson for kindly providing salinity data and for field support; Adela Dumitrascu and Alexandra Walsh for assistance in the field; Olivia De Meo and Shelly Carpenter for assis-

tance in voyage preparation, sample analysis, and data quality control; and Christian Katlein for insightful comments on the manuscript. Custom saw blades for sectioning the sea ice were kindly provided by Paul Shemeta of Diggit Garden Tools (Edmonds, WA, USA).

Data availability. All data presented in this paper are publicly available at the NSF Arctic Data Center under the DOIs: doi:10.18739/A2BG2HB5Z and doi:10.18739/A26M3350V.

LITERATURE CITED

Anhaus P, Katlein C, Nicolaus M, Hoppmann M, Haas C (2021) From bright windows to dark spots: Snow cover controls melt pond optical properties during refreezing. Geophys Res Lett 48:e2021GL095369

Arrigo KR (2017) Sea ice as a habitat for primary producers. In: Thomas DN (ed) Sea ice. John Wiley & Sons, London, p 352–369

Belter HJ, Krumpen T, von Albedyll L, Alekseeva TA and others (2021) Interannual variability in Transpolar Drift summer sea ice thickness and potential impact of Atlantification. Cryosphere 15:2575–2591

Boetius A, Albecht S, Bakker K, Bienhold C and others (2013) Export of algal biomass from the melting Arctic sea ice. Science 339:1430–1432

Bowman JS, Rasmussen S, Blom N, Deming JW, Rysgaard S, Sicheritz-Ponten T (2012) Microbial community structure of Arctic multiyear sea ice and surface seawater by 454 sequencing of the 16S RNA gene. ISME J 6:11–20

Castellani G, Losch M, Lang BA, Flores H (2017) Modeling Arctic sea-ice algae: physical drivers of spatial distribution and algae phenology. J Geophys Res 122: 7466–7487

Castellani G, Schaafsma FL, Arndt S, Lange BA and others (2020) Large-scale variability of physical and biological sea-ice properties in polar oceans. Front Mar Sci 7:536

Childers VA, Brozena JM (2005) Long-range aircraft as an Arctic Oceanographic platform. Deep Sea Res I 52: 2366–2375

Cimoli E, Meiners KM, Lund-Hansen-Hansen LC, Lucieer V (2017) Spatial variability in sea-ice algal biomass: an under-ice remote sensing perspective. Adv Polar Sci 28: 268–296

Comiso J (2010) Polar oceans from space. Springer, New York, NY

Cooper ZS, Rapp JZ, Carpenter SD, Iwahana G, Eicken H, Deming JW (2019) Distinctive microbial communities in subzero hypersaline brines from Arctic coastal sea ice and rarely sampled cryopegs. FEMS Microbiol Ecol 95: fiz166

Cox GFN, Weeks WF (1983) Equations for determining the gas and brine volumes in sea-ice samples. J Glaciol 29: 306–316

Dalman LA, Else BGT, Barber D, Carmack E and others (2019) Enhanced bottom-ice algal biomass across a tidal strait in the Kitikmeot Sea of the Canadian Arctic. Elem Sci Anthropocene 7:22

Deming JW, Collins RE (2017) Sea ice as a habitat for bacteria, archaea and viruses. In: Thomas DN (ed) Sea ice. John Wiley & Sons, London, p 326–351

Doney SC, Fabry VJ, Feely RA, Kleypas JA (2009) Ocean acidification: the other CO_2 problem. Annu Rev Mar Sci 1:169–192

DuBois M, Gilles KA, Hamilton JK, Rebers PA, Smith F (1956) Colorimetric method for determination of sugars and related substances. Anal Chem 28:350–356

Fernández-Méndez M, Katlein C, Rabe B, Nicolaus M and others (2015) Photosynthetic production in the Central Arctic during the record sea-ice minimum in 2012. Biogeosciences 12:3525–3549

Firth E, Carpenter SD, Sørensen HL, Collins ER, Deming JW (2016) Bacterial use of choline to tolerate salinity shifts in sea-ice brines. Elem Sci Anthropocene 4:000120

Fransson A, Chierici M, Miller LA, Carnat G and others (2013) Impact of sea-ice processes on the carbonate system and ocean acidification at the ice-water interface of the Amundsen Gulf, Arctic Ocean. J Geophys Res 118: 7001–7023

Gardner WD, Richardson MJ, Smith WO Jr (2000) Seasonal build-up and loss of POC in the Ross Sea. Deep Sea Res II 47:3423–3450

Geider RJ, Macintyre HL, Kana TM (1998) A dynamic regulatory model of phytoplanktonic acclimation to light, nutrients, and temperature. Limnol Oceanogr 43: 679–694

Geilfus NX, Carnat G, Papakyriakou T, Tison JL and others (2012) Dynamics of pCO_2 and related air–ice CO_2 fluxes in the Arctic coastal zone (Amundsen Gulf, Beaufort Sea). J Geophys Res 117:C00G10

Gosselin M, Levasseur M, Wheeler PA, Horner RA, Booth BC (1997) New measurements of phytoplankton and ice algal production in the Arctic Ocean. Deep Sea Res II 44: 1623–1644

Gradinger R (1999) Integrated abundance and biomass of sympagic meiofauna in Arctic and Antarctic pack ice. Polar Biol 22:169–177

Gradinger R (2009) Sea ice algae: major contributors to primary production and algal biomass in the Chukchi and Beaufort Seas during May/June 2002. Deep Sea Res II 56:1201–1212

Gradinger R, Zhang Q (1997) Vertical distribution of bacteria in Arctic sea ice from the Barents and Laptev Seas. Polar Biol 17:448–454

Granfors A, Karlsson A, Mattsson E, Smith WO Jr, Abrahamsson K (2013) Biogenic halocarbons in young Arctic sea ice and frost flowers. Mar Chem 155:124–134

Kashiwase H, Ohshima KI, Nihashi S, Eicken H (2017) Evidence for ice–ocean albedo feedback in the Arctic Ocean shifting to a seasonal ice zone. Sci Rep 7:8170

Kohlbach D, Graeve M, Lange BA, David C, Peeken I, Flores H (2016) The importance of ice algae-produced carbon in the central Arctic Ocean ecosystem: food web relationships revealed by lipid and stable isotope analyses. Limnol Oceanogr 61:2027–2044

Kohlbach D, Lange BA, Schaafsma FL, David C and others (2017) Ice algae-produced carbon is critical for overwintering of Antarctic krill *Euphausia superba*. Front Mar Sci 4:310

Krumpen T, Belter HJ, Boetius A, Damm E and others (2019) Arctic warming interrupts the Transpolar Drift and affects long-range transport of sea ice and ice-rafted matter. Sci Rep 9:5459

Kuwae T, Hosokawa Y (1999) Determination of abundance and biovolume of bacteria in sediments by dual staining with 4′,6-diamidino-2-phenylindole and acridine orange:

relationship to dispersion treatment and sediment characteristics. Appl Environ Microbiol 65:3407–3412

Kwok R, Cunningham GF (2015) Variability of Arctic sea ice thickness and volume from CryoSat-2. Philos Trans R Soc A 373:20140157

Kwok R, Cunningham GF, Kacimi S, Webster MA, Kurtz NT, Petty AA (2020) Decay of the snow cover over Arctic sea ice from ICESat-2 acquisitions during summer melt in 2019. Geophys Res Letters 47:e2020GL088209

Lange BA, Katlein C, Castellani G, Fernández-Méndez M, Nicolaus M, Peeken I, Flores H (2017) Characterizing spatial variability of ice algal chlorophyll *a* and net primary production between sea ice habitats using horizontal profiling platforms. Front Mar Sci 4:349

Lee S, Fuhrman J (1987) Relationships between biovolume and biomass of naturally derived marine bacterioplankton. Appl Environ Microbiol 53:1298–1303

Leppäranta M, Manninen T (1988) The brine and gas content of sea ice with attention to low salinities and high temperatures. Internal Report. Finnish Institute for Marine Research, Helsinki

Lewis KM, van Dijken GL, Arrigo KR (2020) Changes in phytoplankton concentration now drive increased Arctic Ocean primary production. Science 369:198–202

Lund-Hansen LC, Markage S, Hancke K, Stratmann T, Rysgaard S, Ramløv H, Sorrell BK (2015) Effects of sea-ice light attenuation and CDOM absorption in the water below the Eurasian sector of central Arctic Ocean (>88° N). Polar Res 34:23978

Lund-Hansen LC, Hawes I, Hancke K, Salmansen N, Nielsen JR, Balslev L, Sorrell BK (2020) Effects of increased irradiance on biomass, photobiology, nutritional quality, and pigment composition of Arctic sea ice algae. Mar Ecol Prog Ser 648:95–110

Mills MM, Brown ZW, Laney SR, Ortega-Retuerta E, Lowry KE, van Dijken G, Arrigo KR (2018) Nitrogen limitation of the summer phytoplankton and heterotrophic prokaryote communities in the Chukchi Sea. Front Mar Sci 5:362

Mortenson E, Hayashida H, Steiner N, Monahan A and others (2017) A model-based analysis of physical and biological controls on ice algal and pelagic primary production in Resolute Passage. Elem Sci Anthropocene 5:39

Nicolaus M, Perovich DK, Spreen G, Granskog MA and others (2022) Overview of the MOSAiC expedition: snow and sea ice. Elem Sci Anthropocene 10:000046

Notz D, Worster MG (2009) Desalination processes of sea ice revisited. J Geophys Res 114:C05006

Piontek J, Galgani L, Nöthig EM, Peeken I, Engel A (2021) Organic matter composition and heterotrophic bacterial activity at declining summer sea ice in the central Arctic Ocean. Limnol Oceanogr 66:S343–S362

Randelhoff A, Holding J, Janout M, Sejr MK, Babin M, Tremblay JE, Alkire M (2020) Pan-Arctic Ocean primary production constrained by turbulent nitrate fluxes. Front Mar Sci 7:150

Ross PS, Chastain S, Vassilenko E, Etemadifar A and others (2021) Pervasive distribution of polyester fibres in the Arctic Ocean is driven by Atlantic inputs. Nat Commun 12:106

Roy RN, Roy LN, Vogel KM, Porter-Moore C and others (1993) The dissociation constants of carbonic acid in seawater at salinities 5 to 45 and temperatures 0 to 45°C. Mar Chem 44:249–267

Rysgaard S, Glud RN, Sejr MK, Bendtsen J, Christensen PB (2007) Inorganic carbon transport during sea ice growth and decay: a carbon pump in polar seas. J Geophys Res 112:C03016

Snoeijs-Leijonmalm P, Gjøsæter H, Ingvaldsen RB, Knutsen T and others (2021) A deep scattering layer under the North Pole pack ice. Prog Oceanogr 194:102560

Søgaard DH, Thomas DN, Rysgaard S, Glud RN and others (2013) The relative contributions of biological and abiotic processes to carbon dynamics in subarctic sea ice. Polar Biol 36:1761–1777

Spreen G, Kaleschke L, Heygster G (2008) Sea ice remote sensing using AMSR-E 89-GHz channels. J Geophys Res Oceans 113:C02S03

Tedesco L, Vicchi M, Scoccimarro E (2019) Sea-ice algal phenology in a warmer Arctic. Sci Adv 5:eaav4830

Terhaar J, Lauerwald R, Regnier P, Gruber N, Bopp L (2021) Around one third of current Arctic Ocean production sustained by rivers ad coastal erosion. Nat Commun 12:169

Thompson T (2021) Arctic sea ice hits 2021 minimum. Nature doi:10.1038/d41586-021-02649-6

Torstensson A, Young JN, Carlson LT, Ingalls AE, Deming JW (2019) Use of exogenous glycine betaine and its precursor choline as osmoprotectants in Antarctic sea-ice diatoms. J Phycol 55:663–675

Torstensson A, Margolin AR, Showalter GM, Smith WO Jr and others (2021) Sea-ice microbial communities in the central Arctic Ocean: limited responses to short-term pCO_2 perturbations. Limnol Oceanogr 66:S383–S400

Tucker WB, Gow AJ, Meese DJ, Boworth HW (1999) Physical characteristics of summer sea ice across the Arctic Ocean. J Geophys Res 104:1489–1504

van Heuven SMAC, Pierrrot D, Rae JWB, Lewis E, Wallace DWR (2011) MATLAB program developed for CO_2 system calculations, ORNL/CDIAC-105b. Carbon Dioxide Information Analysis Center, Oak Ridge National Laboratory, US Department of Energy, Oak Ridge, TN

Warner K, Iacozza J, Scharien R, Barber D (2013) On the classification of melt season first-year and multi-year sea ice in the Beaufort Sea using Radarsat-2 data. Int J Remote Sens 34:3760–3774

Welschmeyer NA (1994) Fluorometric analysis of chlorophyll *a* in the presence of chlorophyll *b* and pheopigments. Limnol Oceanogr 39:1985–1992

Editorial responsibility: Toshi Nagata, Kashiwanoha, Japan
Reviewed by: 3 anonymous referees

Submitted: March 31, 2022
Accepted: November 10, 2022
Proofs received from author(s): December 18, 2022